Direct Determination of the Local Structure in Molten Alumina by High Temperature X-Ray Diffraction

Y. Waseda [a], K. Sugiyama [a], and J. M. Toguri [b]

[a] Institute for Advanced Materials Processing (SOZAIKEN) Tohoku University, Sendai 980-77, Japan
[b] Department of Metallurgy and Materials Science University of Toronto, Toronto, Ontario M5S 1A4, Canada

Z. Naturforsch. **50a**, 770–774 (1995); received March 18, 1995

A high temperature X-ray diffraction study of molten alumina has been carried out at 2363 K (2090 °C). The local ordering parameters in molten alumina were estimated by using the interference function refining technique. Octahedrally coordinated aluminum is suggested to remain in the melt as the fundamental local structure.

1. Introduction

Alumina is well-recognized as a reference material used in various high temperature measurements [1]. For example, the enthalpy value of liquid alumina is often taken as a criterion for calibrating high temperature calorimeters. The properties of molten alumina are also of practical importance. For example, their knowledge is essential for industrial application in materials processing such as the sintering reaction for producing new functional ceramics [2]. In addition, there is an increasing need for understanding various thermophysical properties, including the atomic scale structure of molten alumina which is quite limited [3].

The main purpose of this paper is to present the structural data of molten alumina obtained by means of high temperature X-ray diffraction.

2. Experimental Procedure

The present experimental arrangement, using a theta-theta diffractometer with a high temperature, chamber which allowed the sample to be held in a stationary horizontal position, was almost identical to that employed previously for molten oxide systems [4, 5]. Therefore, only the essential features are summarized here; A high temperature cell made from a molybdenum plate ($70 \times 20\ mm^2$, thickness $0.2 \sim 0.5$ mm) was used both as heater and sample container. The sample in powder form was packed into a container ($20 \times 15 \times 5\ mm^3$) which was part of the main heater. In addition, a 3 mm mesh molybdenum net was placed on the sample surface. This resulted in the spreading of the molten sample through the mesh to form an approximately flat surface due to surface tension effects. This sample holder-heater assembly was set in the high temperature chamber [6]. An additional heating element was also directed to the top surface of the sample in order to insure a uniform sample temperature. Figure 1 shows schematically the sample holder-heater assembly.

The molten sample was prepared from high purity alumina powder of 99% purity (Wako Pure Chemical Industries, Ltd). The sample was melted in this assembly using a 160 A and 12 V input power source under a purified dry argon atmosphere. The sample temperature was monitored with a W/5Re-W/26Re thermocouple which was spot-welded to the bottom of the sample holder. The thermocouple readings showed agreement with the melting points of pure platinum and rhodium within ± 6 K. However, optical pyrometer readings made through the top sight hole of the chamber indicated differences from the thermocouple readings by amounts of the order of ± 22 K at 2000 K. This may be due to high radiation losses from the sample and absorption in the sight hole windows. For this reason, the sample temperature was calibrated by measuring the lattice parameter of molybdenum powder packed into the mesh of the net and by comparing the change in lattice parameter with the thermal expansion data of pure molybdenum [6]. This method of calibration makes it possible to maintain the sample temperature to within ± 10 K.

Reprint requests to Prof. Y. Waseda.

0932-0784 / 95 / 0800-0770 $ 06.00 © – Verlag der Zeitschrift für Naturforschung, D-72027 Tübingen

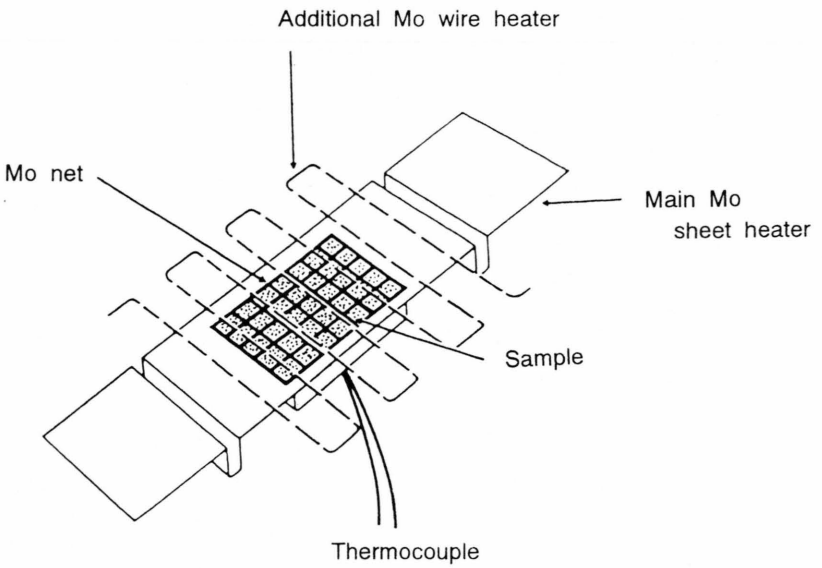

Fig. 1. Schematic diagram of sample holder-heater assembly employed in this work for the high temperature melt.

The X-ray scattering intensities were measured at 2363 K using Mo $K\alpha$ radiation coupled with a singly-bent pyrolitic graphite monochromator in the diffracted beam. The intensity profile was obtained in an angular range from 2° to 75°, which corresponds to wave vectors $Q=4\pi\sin\theta/\lambda$ of 6 to 170 nm^{-1}, where λ is the wave length and θ is half the scattering angle. The observed intensity data at $Q\leq 6\ nm^{-1}$ were smoothly extrapolated to zero at $Q=0\ nm^{-1}$. It may be noted that the effect of this extrapolation or truncation up to $Q=170\ nm^{-1}$ for the broad peaks as detected in a liquid sample is known to make no critical contribution to the radial distribution function analysis [7].

3. Data Processing

The method of analyzing the measured X-ray scattering intensity data for non-crystalline systems such as liquids and glasses is well established and has been described in detail in [8–10]. Consequently, only the essential equations and their relevance are given here for convenience of discussion.

For structural studies of non-crystalline systems containing more than one kind of atom the concept of units of composition (uc's) is frequently used [8–10]. In the present case, the feasible units would be two aluminum and three oxygen atoms. As a result, the reduced interference function for the uc's $i(Q)$, as a function of the wave vector, which is related to the structurally sensitive part of the X-ray scattering intensity per uc, $I_{eu}(Q)$, is given by the equation

$$i(Q)=\frac{I_{eu}(Q)/N-\sum_{uc}f_j^2}{f_e^2}, \tag{1}$$

where f_j and f_e are the usual atomic scattering factor and the average scattering factor per electron, respectively. The electron RDF can be readily estimated from the interference function data by the following Fourier transformation;

$$\mathrm{RDF}_{exp}=2\pi^2 r\varrho_e\sum_{uc}Z_j+\int_0^{Q_{max}}Q\,i(Q)\sin Q r\,dQ, \tag{2}$$

where ϱ_e is the average number density of electrons and Z_j is the atomic number of element j.

4. Results and Discussion

Figure 2 shows the reduced interference function, $Q\,i(Q)$, for molten alumina at 2363 K obtained from the present measured X-ray scattering intensity data. The electron RDF of molten alumina calculated from the interference function of Fig. 2, using (2) together with the density value of 3.01 Mg/m^3 [11], is shown in Figure 3.

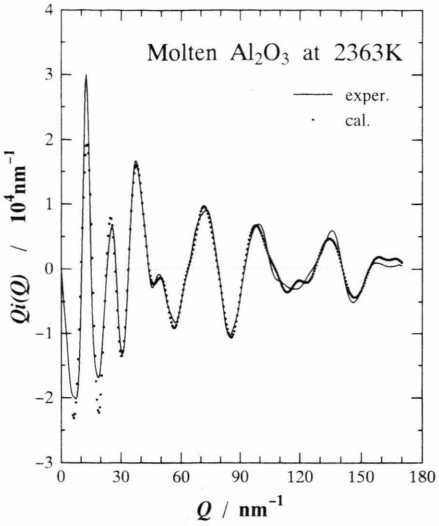

Fig. 2. Reduced Interference function $Qi(Q)$ of molten alumina at 2363 K. Solid lines: experimental data, Dotted lines: calculation by (3).

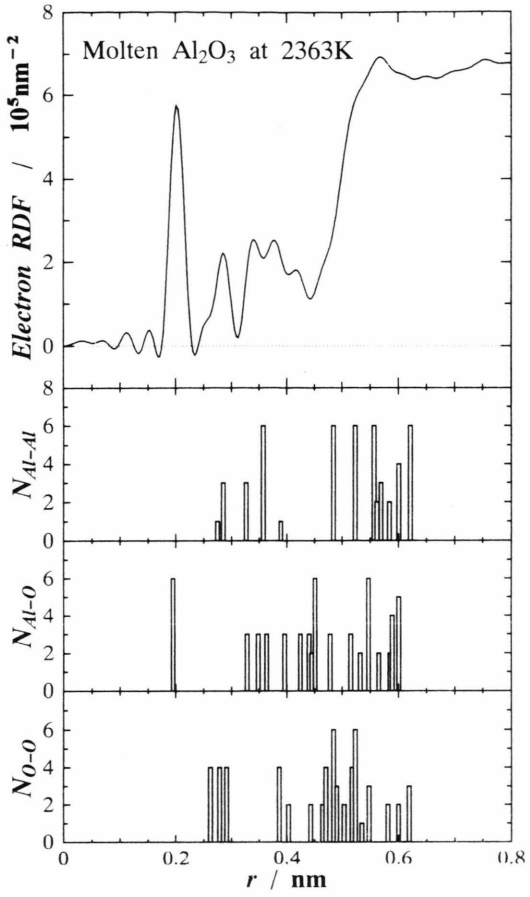

Fig. 3. Electron radial distribution function (RDF) of molten alumina at 2363 K. Solid lines: experimental data, Histograms: the interatomic distance found in crystalline α–Al_2O_3 [16].

The exact estimation of the experimental uncertainty in the structural analysis of a molten sample, particularly for the measurement at high temperatures over 1273 K (1000 °C) by X-ray diffraction, is known to be technically difficult. Nevertheless, the experimental uncertainty in the present structural data has been evaluated as follows.

The accumulated intensity counts were about 10^4 around the first peak region and about 5×10^3 in other regions, in order to hold the counting statistics approximately uniform. Systematic errors in X-ray diffraction arises from the normalization procedure of the measured intensity data and the uncertainty in the atomic scattering factors and Compton scattering intensities [12]. Such errors can be estimated by a procedure recommended by Greenfield et al. [13] and Rahman [14]. Following their method, the total error in the interference function obtained in this work is estimated to be about 4%. The uncertainty of the RDFs is probably similar to that of the interference function because the computational errors were minimized by employing the accepted procedures in the Fourier transformation [15]. In addition, it is necessary to take into consideration that the present measurements can be affected by the inherent difficulties arising from the high temperatures over 2000 K. Thus, some reservation is attached to the accuracy of the present structural information, which is lower than those associated with investigations on molten metals and oxides at temperatures below 1273 K [9].

Figure 2 shows the reduced interference function $Qi(Q)$ of liquid alumina. The general features of the function $Qi(Q)$ are similar to that of typical molten oxides. Namely, the interference function of molten alumina has a relatively sharp first peak at $Q=13$ nm^{-1}, followed by a number of smaller and broader peaks, which is in contrast to cases of metallic samples where the damping behavior of the function is rapid and monotonic [9]. This indicates that a considerable fraction of local ordering remains in this molten sample although its distribution appears to have no long range ordering.

The electron RDF is given in Figure 3. The histograms at the bottom of Fig. 3 denote the average

distances of some pairs of the α–Al_2O_3 structure at 2070 K [16]. The first peak at around 0.20 nm is attributed to the Al–O pair and the second one around 0.28 nm to a combination of O–O and Al–Al pairs. Apparently the essential features of the atomic arrangement in the molten state are similar to those in the α–Al_2O_3 structure. This also leads to the suggestion that the interference function refining technique with the random vacancy model of α–Al_2O_3 structure can be used for estimating the structural parameters in the near neighbour region of molten alumina.

The interference function refining technique is based on the contrast between local ordering and complete loss of positional correlations at longer distances [9, 17]. Oxide melts belong to this category. These characteristic structural features may be provided by the following expression with respect to the interference function [18]:

$$Qi(Q) = \sum_{j=1}^{m} \sum_{k} c_j \frac{f_j f_k N_{jk}}{f_e^2 r_{jk}} \exp(-\sigma_{jk} Q^2) \sin(Q r_{jk}) + \sum_{\alpha=1}^{m} \sum_{\beta=1}^{m} c_\alpha c_\beta \frac{f_\alpha f_\beta}{f_e^2} \exp(-\sigma'_{\alpha\beta} Q^2) \cdot 4\pi \varrho_0 \frac{Q r'_{\alpha\beta} \cos(Q r'_{\alpha\beta}) - \sin(Q r'_{\alpha\beta})}{Q^2}. \quad (3)$$

The first term on the right-hand side of (3) corresponds to the discrete Gaussian like distribution of near neighbors with a mean-square variation $2\sigma_{ik}$, while the second term provides the distribution for higher neighbor correlations approximated by a continuous distribution with the average number density of the system. The quantities $r'_{\alpha\beta}$ and $\sigma'_{\alpha\beta}$ are the parameters of the boundary region between the discrete distribution in the near neighbor region and the continuous one at longer distances. It should be noted that these two parameters need not be sharp [17]. By applying (3), the values of the coordination number N_{jk} and interatomic distance r_{jk} for near neighbor correlations can be estimated using a least-squares analysis so as to fit the experimental interference function by iteration. This interference function refining technique has frequently been used for structural investigations of inorganic liquids and glasses. The variation in the coordination number in this analysis does not exceed ± 0.5. However, this technique is not a unique mathematical procedure but a semi-empirical one for the resolution of the peaks in the RDF of non-crystalline systems. Thus, the application is effective only for a few near neighbor correlations.

Table 1. Structural parameters of liquid Al_2O_3.

Pair	Molten Al_2O_3 at 2363 K		α–Al_2O_3 at 2170 K	
	nm	atom	nm	atom
Al–O	0.202	5.6	0.188	3.0
			0.202	3.0
O–O	0.282	6.2	0.258	2.0
			0.267	2.0
			0.278	4.0
			0.291	4.0
Al–Al	0.287	2.3	0.274	1.0
			0.285	3.0

The dotted line in Fig. 2 is the resultant interference function with the initial structural parameters obtained from the random vacancy model of α–Al_2O_3 with the density value of 3.01 Mg/m^3. The agreement is satisfactory, and thus the structural parameters obtained in this analysis are acceptable. The converged structural parameters of molten alumina in the near neighbor region are summarized in Table 1, together with those of crystalline α–Al_2O_3 [16].

The interatomic distance for the first neighboring Al–O in molten alumina is estimated to be 0.202 nm. This value corresponds to the octahedral coordination formed by six oxygens, while the value is 0.18 nm for the tetrahedral arrangement [19]. This is also supported by the obtained coordination number of 5.6 around aluminum for this Al–O correlation. It is well known for the near neighbor correlations in the α–Al_2O_3 crystalline structure that the aluminum is surrounded by four aluminums (one at 0.274 nm and three at 0.285 nm). However, the coordination number for the first neighboring Al–Al pair of molten alumina is 2.3 which is rather smaller than that of crystalline α–Al_2O_3. This contrasts to the molten SiO_2 case where the coordination number for Si–Si is 4.0 and agrees with the corresponding crystalline structures of crystoballite or quartz [9, 19]. This difference may be attributed to the relatively large change in the density of alumina on melting, which induces appreciable modification to the near neighbor atomic correlations such as the octahedrally coordinated aluminum. Thus, the atomic arrangement of crystalline α–Al_2O_3 based on hexagonal close packed oxygens alters considerably in order to form a loose structural unit of low density. By considering the present X-ray diffraction results, a three dimensional structural model illustrated in Fig. 4 is proposed as one of the

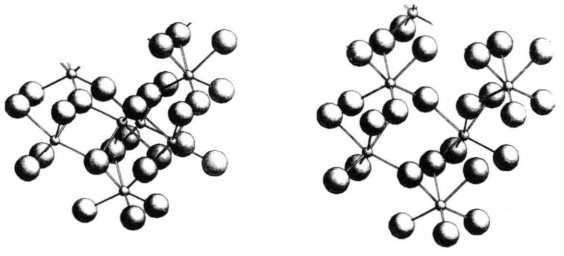

α–Al_2O_3 molten Al_2O_3

Fig. 4. Diagram of the local atomic arrangements in α–Al_2O_3 and molten alumina estimated from the present X-ray diffraction.

possible local atomic arrangements in molten alumina.

A detailed structural model of molten alumina has not been established yet. Nevertheless, the authors believe that the present structural information represents an effort to further the understanding of the structural aspects of oxide systems containing Al_2O_3.

Acknowledgements

This work was carried out as part of a research project, financially supported by a Grant-in-Aid for Scientific Research (B) (No. 06452308) from the Ministry of Education, Science and Culture of Japan.

[1] IUPAC Report of Task Force on Secondly Temperature Standards, Rev. Inst. Hautes Temp. et Refact. **7,** 5 (1970).
[2] W. D. Kingary, Introduction to Ceramics, John Wiley, New York 1960.
[3] A. Nukui, H. Tagai, H. Morikawa, and S. Iwai, J. Amer. Ceram. Soc. **59,** 534 (1976).
[4] Y. Waseda and J. M. Toguri, Met. Trans. **9B,** 595 (1978).
[5] In-Kook Suh, K. Sugiyama, Y. Waseda, and J. M. Toguri, Z. Naturforsch. **44a,** 580 (1989).
[6] Y. Waseda, K. Hirata, and M. Ohtani, High Temp. High Pressure **7,** 221 (1975).
[7] K. Furukawa, Rep. Progr. Phys. **25,** 395 (1962).
[8] H. P. Klug and L. E. Alexander, X-ray Diffraction Procedures for Polycrystalline and Amorphous Materials, (2nd Edition), John-Wiley & Sons, New York 1974.
[9] Y. Waseda, The Structure of Non-Crystalline Materials, McGraw-Hill, New York (1980).
[10] B. E. Warren, X-ray Diffraction, Addison-Wesley Reading, Massachusetts, 1969.
[11] E. E. Shpil'rain, K. A. Yakimovich, and A. F. Tsitsakin, High Temp. High Pressure **5,** 191 (1973).
[12] International Tables for X-ray Crystrallography, Vol. IV, Kynoch, Birmingham 1974.
[13] A. J. Greenfield, J. Wellendorf, and N. Wiser, Phys. Rev. **A4,** 1607 (1971).
[14] A. Rahman, J. Chem. Phys. **42,** 3540 (1965).
[15] R. Kaplow, S. L. Strong, and B. L. Averbach, Phys. Rev. **138,** A1336 (1965).
[16] N. Ishizawa, T. Miyata, I. Minato F. Marumo, and S. Iwai, Acta Crystallogr. **B36,** 228 (1980).
[17] A. H. Narten, J. Chem. Phys. **56,** 1905 (1972).
[18] L. Pauling, The Nature of the Chemical Bond, Cornell Univ. Press., Ithaca 1945.
[19] K. Sugiyama, E. Matsubara, I. K. Shu, Y. Waseda, and J. M. Toguri, Sci. Report, RITU **A34,** 143 (1989).